JOURNAL OF CATALYSIS 26, 153–162 (1972)

Reaction Network and Kinetics of p-Diethylbenzene Cracking Over X-Faujasite Molecular Sieve Catalysts

L. FORNI AND S. CARRÀ

Istituto di Chimica Fisica, Università di Milano, Milan;
Istituto di Chimica Fisica, Università di Bologna, Bologna, Italy

Received May 3, 1971

The catalytic behaviour of a set of partially decationated Na-X-zeolites has been tested for *p*-diethylbenzene cracking reactions in the temperature range of 500 to 568°C. A large spectrum of reaction products, deriving from isomerization, dealkylation, dehydrogenation and hydrodealkylation, has been detected and a reaction network consistent with a kinetic analysis of the products distribution is offered. An analysis of the relative influence of radical and ionic contribution to the reaction products formation is also given.

INTRODUCTION

The study of hydrocarbon cracking reactions over sodium-X-zeolites presents a particular interest, due to their ability of promoting a radical chain mechanism (*1*). In fact the surface of the catalyst can initiate radical reactions with the formation of molecular active centers, which give rise to a chain mechanism, analogous to the one developed by Kossiakoff and Rice (*2*).

Actually over partially decationated X-zeolites both a radical and an ionic mechanism can occur and the evaluation of the amount of the two processes can be derived from a careful analysis of reaction products. In the present work *p*-diethylbenzene (*p*-DEB) has been employed as reactant on a set of partially decationated NaX zeolites. A wide range of reaction products was observed and detected. Such an analysis allowed the formulation of some reasonable hypotheses on the relative influence of radical and ionic mechanisms.

EXPERIMENTAL METHODS

Reagents. *p*-DEB was prepared from ethylbenzene through *p*-ethylacetophenone, according to Mowry, Renoll, and Huber (*3*) and Huang-Minlon (*4*). Its purity, tested by gas chromatography, was >99.7%, the remaining part being the *m*- and *o*-isomers. The purity of nitrogen was >99.999%.

Catalysts. Partially decationated 30–60 mesh Linde 13X molecular sieves have been employed as catalysts. The decationation has been performed following the technique suggested by Breck *et al.* (*5*), by exchanging part of the original Na^+ cations with NH_4^+ and then gradually heating the exchanged zeolites in a tubular furnace up to 570°C for 3 hr in a slow flow of dry nitrogen. The analysis of exchanged zeolites was done by titration of Na^+ and NH_4^+ ions in the exchanging solutions and by determination of the residual Na^+ in the decationated zeolites, after disintegration with concentrated HCl. Four catalysts were prepared, whose percentages of exchanged Na^+ ions, with respect to the total Na^+ present in the original zeolite, were the following:

Catalyst type	Exchanged Na^+ (%)
A	15.7
B	21.6
C	26.1
D	41.2

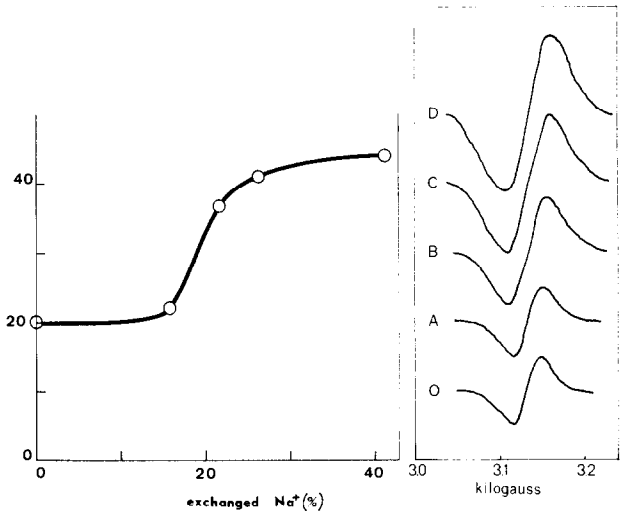

FIG. 1. Increase of spin density (arbitrary units) of the catalyst samples vs decationation degree.

An X-ray analysis (Debye method) ensured that the crystalline structure of the zeolite had not collapsed in any of our catalysts, even for the highest exchanging percentages.

ESR spectra were recorded for all the prepared catalysts, by means of a Varian, X-band, Model 4502 EPR spectrometer. Spectra were obtained at room temperature and the relative ESR sensitivity for the different catalysts was measured. It was found that the spin densities depend on decationation as shown in Fig. 1.

Apparatus. The kinetic runs have been performed in a Pyrex glass tubular fixed bed flow microreactor of about 7 mm i.d., surrounded by a sand bath, fluidized by compressed and preheated air, in order to minimize temperature gradients along the catalyst bed. Nitrogen and *p*-DEB, fed, respectively, through a suitable gas metering device and by a positive displacement syringe pump, were mixed and fed to the reactor. After reaction the hot gases passed through a liquid nitrogen trap, in which all the liquid effluent substances were frozen. The reactor was heated by an electrical furnace, driven by an electronic temperature controller-recorder. The catalyst bed temperature constancy was ±1°C. No appreciable temperature fluctuations were recorded along the catalyst bed during all the experimental runs.

Analysis. The analysis of the substances entering and leaving the reactor was made by gas chromatography, employing a Wilkens Aerograph Model 600-C flame ionization detector gas chromatograph, equipped with a copper column, 2 mm i.d., 3 m long, packed with 5% + 5% Bentone 34 + Didecylphthalate on acid-washed 80–100 mesh Chromosorb W (column temp, 97°C; carrier gas, nitrogen 25 ml/min; injected samples, 0.03 μl). A careful determination of analytical correction factors was made in order to ensure precise analytical data even at the lower conversions.

Procedure. All the experimental runs were performed with fresh catalyst as follows. After the catalyst had been introduced into the reactor, the temperature was gradually raised to the chosen value in about 3 hr. When the reactor temperature had reached 300°C, the nitrogen flow was started. The feeding of *p*-DEB was started only about 10 min after the reactor had reached the steady state at the chosen run temperature. Two hours after starting the feeding of the reactant, the first sample of reaction products was taken, controlling and recording all experimental conditions. A second sample was taken from 0.5 to 5 hr after the collection of the first one, in order to check the reproducibility of each experimental result. A small quantity of inhibitor (*p-tert-*

TABLE 1
TYPICAL RUN ANALYSIS

Run no.	29/9
Temp (°C)	500
p-DEB feeding flow rate (moles/hr)	0.0019
N_2 feeding flow rate (moles/hr)	0.1881
Catalyst type	B
Catalyst wt (g)	0.1904
Liquid effluent analysis (moles %)	
Benzene	Trace
Toluene	Trace
Ethylbenzene	0.85
Styrene	Trace
Methylethylbenzene *p*	0.15
m	Trace
o	Trace
Diethylbenzene *p*	97.47
m	Trace
o	—
Ethylvinylbenzene *p*	1.44
m	0.08
o	—

butyl-catechol) was immediately joined to each sample to prevent any polymerization or oxidation before analysis. A typical run analysis is given in Table 1. Some effluent gas samples were also analyzed, in which the presence of methane, ethylene and hydrogen in various amounts was detected, together with small traces of ethane.

EXPERIMENTAL DATA

Preliminary runs. Some preliminary runs were made to ascertain the catalyst activity change during the reaction time. Such runs were made exploring the whole temperature range of our kinetic experiments (500 to 568°C) and at *p*-DEB partial pressure at the feed higher than that of kinetic runs, in order to maximize the effects of activity changes. An example is given in Fig. 2, in which the conversions of *p*-DEB to the major reaction products vs reaction time are reported. One can see that, despite the hydrocarbon partial pressure being 5 times that of kinctic runs, after a small rise during the first hour, the conversion remained constant. Then for all the kinetic runs the samples for the analysis were taken at least 2 hr after the system had reached the steady state conditions, so that

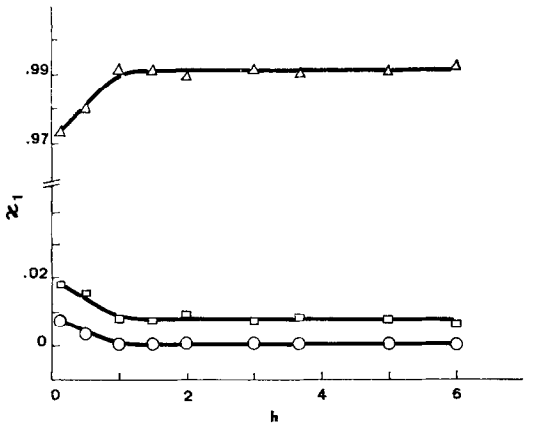

FIG. 2. Conversion vs reaction time. Type B catalyst. T = 530°C, P_w = 0.05 atm, (△) DEB, (□) EVB, (○) EtB.

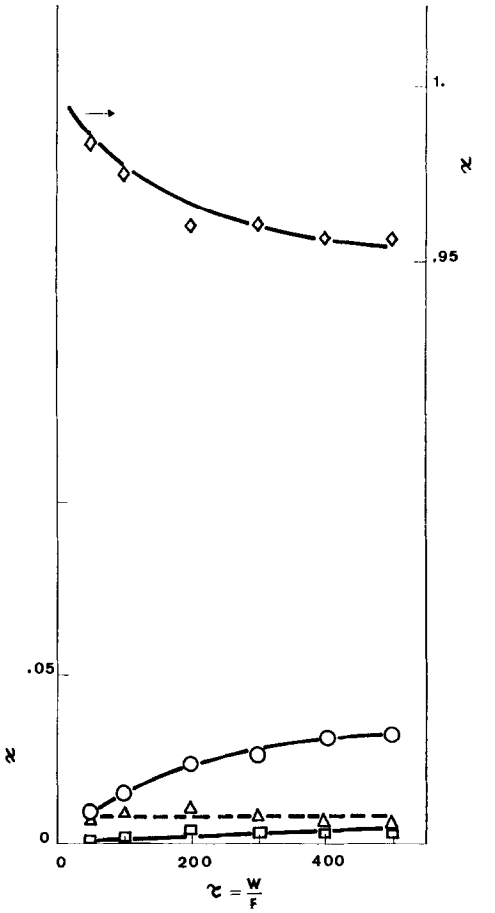

FIG. 3. Conversion vs time factor. T = 500°C, P_w = 0.01 atm, (◇) DEB, (○) EVB, (△) EtB, (□) MEB. (—) from Eqs. (7) and data of Table 2. Type B catalyst.

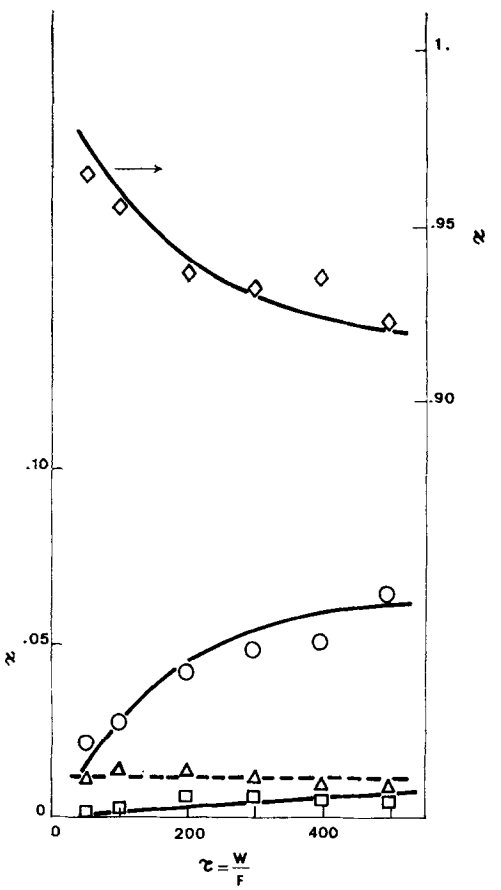

FIG. 4. Conversion vs time factor. T = 530°C; other conditions, symbols and solid lines as in Fig. 3.

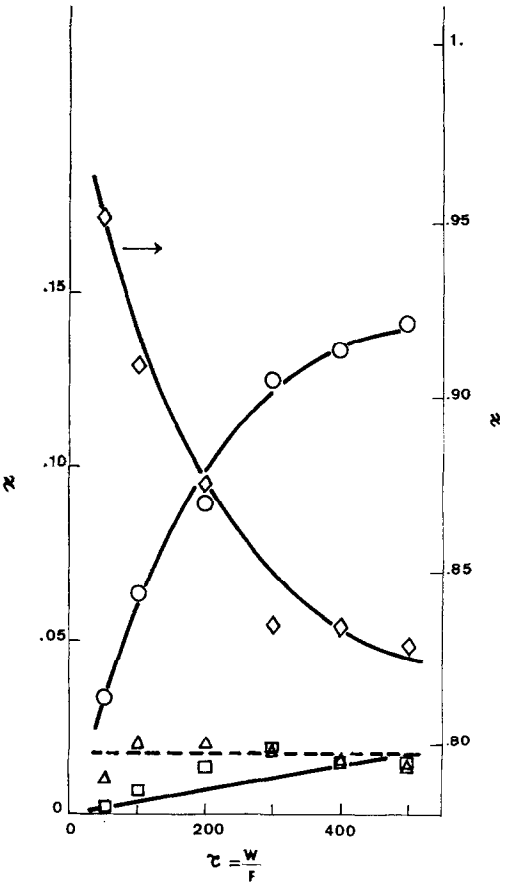

FIG. 5. Conversion vs time factor. T = 568°C; other conditions, symbols and solid lines as in Fig. 3.

the experimental data would correspond to certainly reproducible conditions. Such a reproducibility was confirmed by the duplication of all the experimental data.

Some runs were also made at 568°C employing the original unexchanged sodium zeolite as catalyst. Only very small (almost undetectable) traces of reaction products were found in the reactor effluent during such runs, even at the highest contact times.

Experimental data. A first set of kinetic runs was made at 500, 530 and 568°C and at *p*-DEB partial pressure at the feed of 0.01 atm, employing the type B catalyst. The results are graphically reported in Figs. 3, 4 and 5. A second set of experimental runs has been performed at 568°C and *p*-DEB partial pressure at the feed of 0.01 atm, employing the types A, C and D catalysts. The results are given in Fig. 6, in which the conversion vs exchanged Na^+ percentages in the catalyst is reported.

REACTION KINETICS

Influence of mass transfer (external diffusion). The influence of external diffusion on reaction kinetics was tested by analyzing the values of the ratio $\Delta P_w/P_w$, where ΔP_w is the difference between the *p*-DEB partial pressure in the gas stream (P_w) and at the external surface of the catalyst particles, taken to be roughly spherical, for some suitable chosen kinetic runs. Such a ratio is given by

$$\frac{\Delta P_w}{P_w} = \frac{r}{a_m k_G P_w}, \qquad (1)$$

r being the reaction rate per unit mass of catalyst particle, a_m the external area of

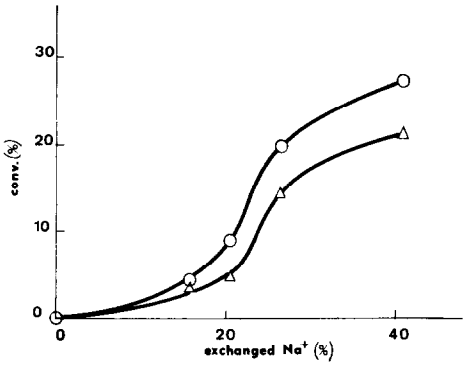

FIG. 6. Conversion vs decationation degree. T = 568°C, P_w = 0.01 atm, (△)τ = 50 (g hr/moles), (○)τ = 100 (g hr/moles).

particles per unit mass of catalyst, k_G the mass transfer coefficient of *p*-DEB, calculated by the well-known *J*-factor correlation (*6*). The diffusion coefficient of *p*-DEB in nitrogen and the viscosity of the gas mixture have been evaluated by the standard procedures (*7*). For the runs performed with type B catalyst, the resulting values of $\Delta P_w/P_w$ were less than 0.008 at any temperature. Therefore the effect of external diffusion was very small and could be neglected.

Influence of internal diffusion. The influence of internal diffusion on reaction kinetics has been analyzed by calculating the value of catalyst effectiveness η in the conditions of maximum reactivity, i.e., 568°C and about 2% conversion. Such a value has been evaluated, following the suggestions of Satterfield (*8*), from the value of the modified Thiele modulus Φ_s, given by

$$\Phi_s = \frac{R^2}{D_{\text{eff}}}\left(-\frac{1}{V_c}\frac{dn}{dt}\frac{1}{c_s}\right) \qquad (2)$$

in which R is the catalyst particle radius (cm), D_{eff} the effective diffusion coefficient for a porous solid, based on total cross section, normal to the direction of diffusion (cm²/sec), V_c the catalyst particle volume (cm³), (dn/dt) the reaction rate (moles/sec), c_s the reactant surface concentration. D_{eff} has been evaluated by the formula:

$$\frac{1}{D_{\text{eff}}} = \frac{1}{D_{K\text{eff}}} + \frac{1}{D_{B\text{eff}}} \qquad (3)$$

where

$$D_{K\text{eff}} = 19400\,\frac{\theta^2}{\tau_f S_g \rho_p}\left(\frac{T}{M}\right)^{1/2} \qquad (4)$$

and

$$D_{B\text{eff}} = D_B\,\frac{\theta}{\tau_f} \qquad (5)$$

θ being the catalyst particle void fraction, τ_f the tortuosity factor, S_g the catalyst surface area (cm²/g), ρ_p the catalyst particle density (g/cm³), T the temperature (°K), M the reactant molecular weight and D_B the bulk diffusion coefficient of the reactant (cm²/sec). For a mean catalyst particle radius of 0.017 cm the calculations gave $D_{\text{eff}} = 0.00207/\tau_f$ and $\Phi_s = 0.1575\tau_f$. Such a value of the modified Thiele modulus Φ_s ensures an almost unitary value of the effectiveness factor η, even if the tortuosity factor would be as high as 10.

Reaction network. The considerable number and the nature of the reaction products present in the reactor effluent suggest the reaction network shown in Fig. 7. The de-

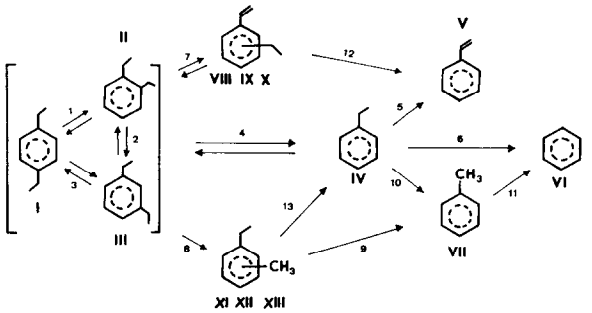

FIG. 7. Complete reaction network.

alkylation reactions can occur through a radical mechanism in which the breaking of the C–C bond is due to the presence of hydrogen deriving from dehydrogenation, with formation of an aromatic compound and a paraffin (hydrodealkylation process). Actually among the reaction products only negligible traces of ethane have been detected with respect to ethylene. Otherwise it is not possible for ethylene to derive from ethane by dehydrogenation, since at the working temperatures the thermodynamic equilibrium favors the hydrogenation reaction of the olefin. Therefore the participation of hydrodealkylation processes takes place only in reactions 8, 10 and 11.

Dealkylation (4, 6, 9, 12) and isomerization (1, 2, 3) reactions occur through an ionic mechanism, in which the hydrogen ions of zeolite are involved, e.g.:

through a radical chain mechanism, whose initiation reactions may be:

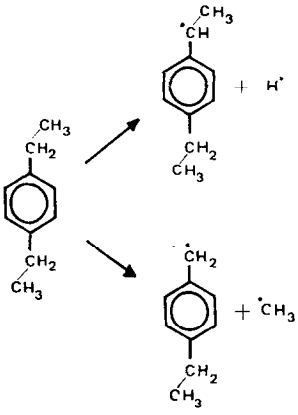

The chain reactions can allow the formation of the detected products as follows.

As a consequence of such an assumption

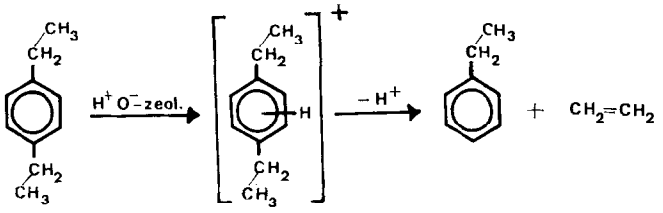

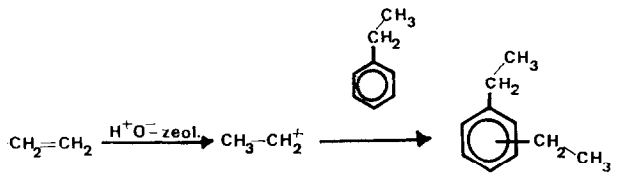

The intervention of the ionic contribution in the dehydrogenation reaction implies a carbonionogenetic splitting of a C–H bond, but, in the case of zeolites, it is largely accepted (*9*) that this model fails to account for the catalytic behavior of such materials. On the contrary, the intervention of a radical-forming process in the mentioned reaction represents a useful model for the correlation of the experimental data and therefore dehydrogenation (5, 7) and hydrodealkylation (8, 10, 11) reactions have been assumed to occur

it is possible to calculate the value of the ionic and of the radical contributions given by the catalyst by simply calculating the sum of the reaction products due to the radical mechanism (V, VII, VIII, IX, X, XI, XII, XIII) and the sum of the reaction products due to the ionic mechanism (II, III, IV, VI). In Fig. 8 the ratio of the two contributions, denoted by (rad/ion), is given as a function of time factor τ, for the runs performed with type B catalyst at the temperatures of 500, 530 and 568°C. The increasing of the curves with the in-

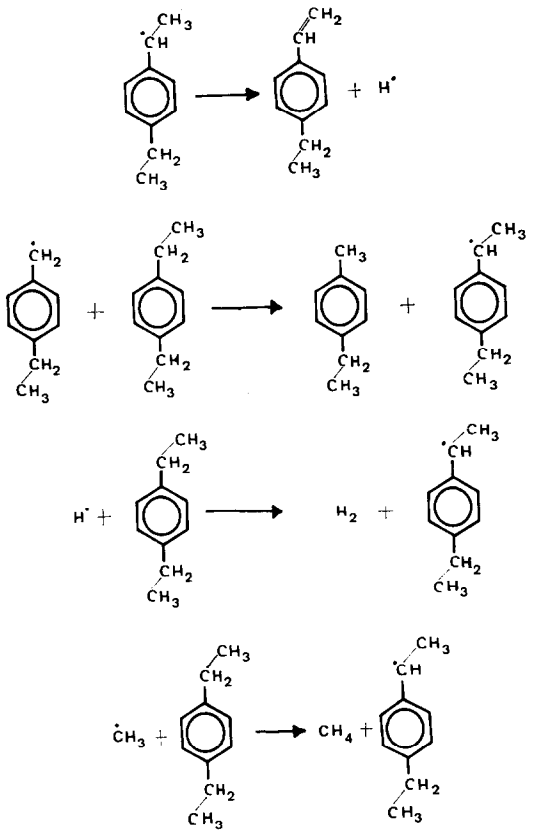

creasing of time factor is due to the fact that the ionic contribution is limited by equilibrium, while the radical contribution is not equilibrium limited. In any case the amount of the influence of temperature on

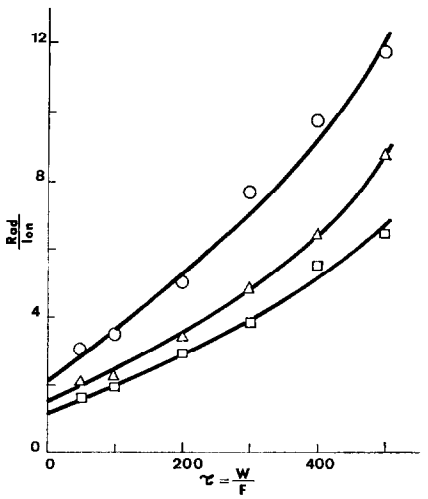

FIG. 8. Rad/ion ratio vs time factor. Type B catalyst, (□) 500°C, (△) 530°C, (○) 568°C.

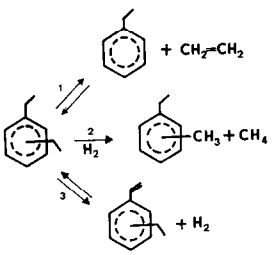

FIG. 9. Simplified reaction network.

the relative influence of the two contributions can be obtained from the intercepts of the curves of Fig. 8; such intercepts are 1.2 at 500°C, 1.5 at 530°C and 2.1 at 568°C.

Kinetic interpretation. Since the concentrations of benzene, toluene and styrene were in any case very small, compared with those of other reaction products, for a kinetic analysis it was possible to simplify the general reaction network of Fig. 7 by neglecting such substances. Then the simplified reaction network of Fig. 9 has been employed. Due to the fact that we are essentially interested in emphasizing the relative importance of dehydrogenation and hydrodealkylation reactions, in this simplified scheme the disubstituted benzene isomers have been considered as single products.

Denoting by x, y, z, w and a the moles of ethylvinylbenzene (EVB), ethylbenzene (EtB), methylethylbenzene (MEB), DEB and nitrogen, respectively, we can write: $n_{DEB} = w$, $n_{EtB} = y$, $n_{MEB} = z$, $n_{EVB} = x$, $n_{H_2} = x - z$, $n_{CH_2=CH_2} = y$, $n_{CH_4} = z$, $n_{N_2} = a$. The mole summation will then be $\Sigma = 1 + x + y + a$, having referred the concentrations to the fed *p*-DEB, i.e., putting $x + y + z + w = 1$. The rate equations describing the simplified scheme of Fig. 9 may then be written:

$$\begin{cases} -\dfrac{dw}{d\tau} = r_1 + r_2 + r_3 - r_{-1} - r_{-3} \\ \dfrac{dy}{d\tau} = r_1 - r_{-1} \\ \dfrac{dz}{d\tau} = r_2 \\ \dfrac{dx}{d\tau} = r_3 - r_{-3}, \end{cases} \tag{6}$$

r_i being the reaction rates (moles/hr g cat)

and $\tau = W/F$ the time factor, where W is the catalyst weight (g) and F the p-DEB feeding rate (moles/hr).

The low value of the reactant partial pressure justifies the employment of pseudo-first order rate equations, so that the reaction rates have been expressed as follows:

$$r_i = k_i P_i,$$

P_i being the partial pressure of the substance i (atm) and k_i the reaction rate constant (moles/hr g atm) referred to the scheme of Fig. 9. Actually an analysis of the experimental data reported in Figs. 4, 5 and 6 reveals that the EtB/DEB ratio is nearly constant and this fact means that, within the considered time factor range, the dealkylation reaction may be taken to be at equilibrium. The experimental mean values of EtB/DEB ratio allowed a direct evaluation of the approximate values of the equilibrium constant K_1 for reaction 1; the Van't Hoff plot of such constants is given in Fig. 11.

By expressing P_i by means of molar fractions and total pressure (1 atm) and introducing the equilibrium constant for the reaction 3, $K_3 = k_3/k_{-3}$, we may write:

$$\begin{cases} \dfrac{dz}{d\tau} = k_2 \dfrac{w}{\Sigma}, \\ \dfrac{dx}{d\tau} = \dfrac{k_3}{\Sigma}\left[w - \dfrac{1}{K_3}\dfrac{x(x-z)}{\Sigma} \right], \end{cases} \tag{7}$$

w has been evaluated by means of the relationship $w = 1 - x - y - z$, which has been taken to be valid only for the range of time factor in which reaction 1 may be assumed to be at equilibrium.

The system (7) of differential equations has been integrated numerically by the Runge-Kutta method, by employing the mean experimental values for y and optimizing, by the steepest descent method, the values of the kinetic constants k_2 and k_3 and of equilibrium constant K_3, i.e., by minimizing the function:

$$F_1(k_2, k_3, K_3) = \sum_{N=1}^{3} \sum_{M=1}^{N} \left[\frac{(C_{N,M} - S_{N,M})^2}{C_{N,M} S_{N,M}} \right], \tag{8}$$

TABLE 2
REACTION RATE AND EQUILIBRIUM CONSTANTS

	500°C	530°C	568°C
k_2 (moles/hr g atm)	0.001	0.0014	0.004
k_3 (moles/hr g atm)	0.017	0.030	0.066
$K_3 \times 10^4$ (atm)	0.105	0.390	2.25

where $C_{N,M}$ is the calculated value of the conversion for the M-th run, performed at the temperature characterized by the subscript N; $S_{N,M}$ is the corresponding experimental result; N is the total number of experimental runs at a given temperature. The application of such a method brings to a minimization of the sum of the squares of the differences between calculated and experimental data. The calculation, performed with a UNIVAC 1108 computer, gave the results reported in Table 2. By means of Eq. (7) and employing the values of the reaction rate and equilibrium constants so obtained, the curves, reported as solid lines in Figs. 3, 4 and 5, have been calculated. In Figs. 10 and 11 the Arrhenius plot for the rate constants and the Van't Hoff plot for the equilibrium constants are shown, respectively. From the best straight-

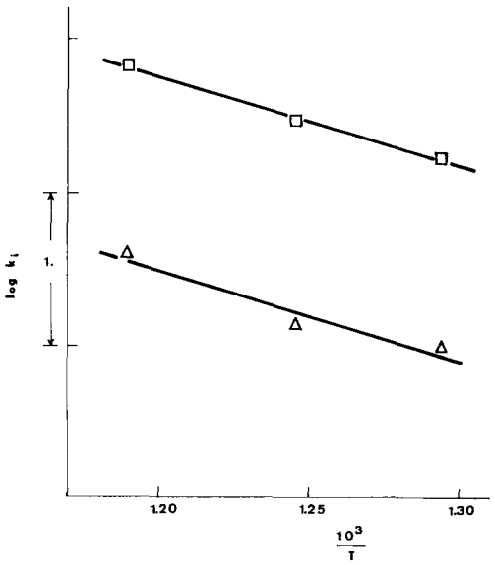

FIG. 10. Arrhenius plot for k_1(○), k_2(△), k_3(□).

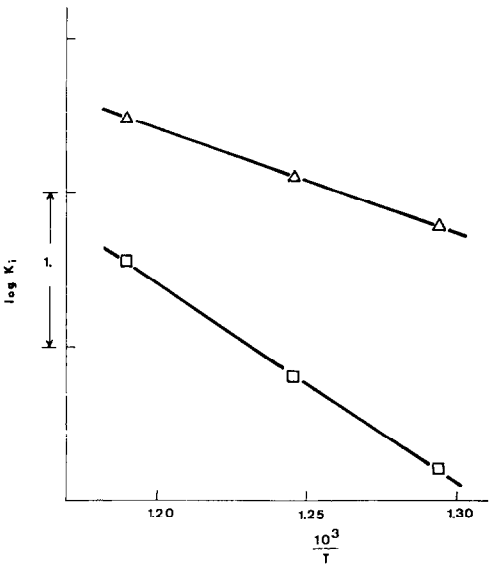

FIG. 11. Van't Hoff plot for $K_1(\triangle)$ and $K_2(\square)$.

line parameters, by means of the well-known equations:

$$\ln k_i = \ln A_i - \Delta E_i^{\neq}/RT, \quad (9)$$

$$\ln K_i = -\Delta H_i^0/RT + \Delta S_i^0/R, \quad (10)$$

the values of the apparent activation energies and of the standard enthalpy and entropy changes of the reactions, reported in Tables 3 and 4, respectively, have been calculated.

DISCUSSION

The present work confirms the possibility of occurrence of two different mechanisms in hydrocarbon cracking over partially decationated Na-X-zeolites. The former is an ionic mechanism, for the explanation of which the carbonium ion concept (*10*) can be applied, the latter is a radical mechanism, in which a radical chain reaction sequence is operative.

Our findings are also consistent with the results of Agudo, Badcock, and Stone (*11*) on the oxidation of hexane isomers. Figure 6 shows that in our experiments the catalytic activity increases by increasing the degree of decationation. It is now interesting to deepen the influence of the decationation degree on the radical contribution. The amount of such contribution for the set of runs reported in Fig. 6 has been evaluated by splitting the total conversion into the two contributions, radical and ionic. The radical contribution is given in Fig. 12 as percentage of converted moles through radical mechanism per hour and per gram of catalyst. It is quite significant that the trend of the curve of Fig. 12 is very similar to that of Fig. 1. This result reveals a narrow correspondence between the catalytic activity due to radical mechanism and the spin density of the catalyst, and seems to confirm that the nonheterogeneous processes are initiated at the zeolite surface. The consistency between the increase of the radical reactions and the increase of ESR signal seems also to give a further justification of the adopted model implying a radical mechanism in the dehydrogenation reaction.

TABLE 3
APPARENT ACTIVATION ENERGIES OF REACTIONS
(SCHEME OF FIG. 10)

$\Delta E_2^{\neq}$ = 26.63 ± 4.48 (kcal/mole)
$\Delta E_3^{\neq}$ = 25.83 ± 0.87 (kcal/mole)

TABLE 4
STANDARD ENTHALPY AND ENTROPY CHANGE OF REACTIONS
(SCHEME OF FIG. 10)

Reaction	$\Delta H°$ (kcal/mole)	$\Delta S°$ (cal/mole °K)
1	58.34 ± 1.53	52.58 ± 1.91
3	31.19 ± 0.12	11.86 ± 0.15

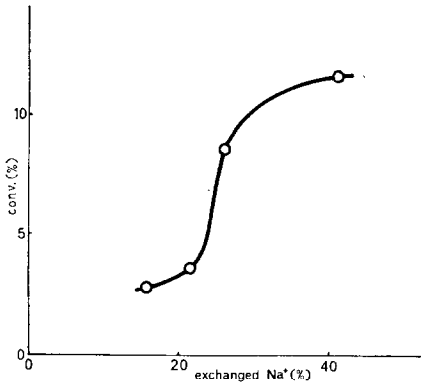

FIG. 12. Contribution of radical mechanism to total conversion vs decationation degree. T = 568C°, P_w = 0.01 atm, τ = 50 (g hr/mnles).

Acknowledgments

We are grateful to Dr. A. Azimonti for valuable help in experimental work and we are indebted to Italian Consiglio Nazionale delle Ricerche for financial aid.

References

1. Frilette, V. J., Weisz, P. B., and Golden, R. L., *J. Catal.* **1**, 301 (1962).
2. Kossiakoff, A., and Rice, F. O., *J. Amer. Chem. Soc.* **65**, 590 (1943).
3. Mowry, D. T., Renoll, M., and Huber, W. F., *J. Amer. Chem. Soc.* **68**, 1107 (1946).
4. Huang-Minlon, *J. Amer. Chem. Soc.* **68**, 2488 (1946).
5. Breck, D. W., Eversole, W. G., Milton, R. M., Reed, T. B., and Thomas, T. L., *J. Amer. Chem. Soc.* **78**, 5963 (1956).
6. Yoshida, F., Ramaswami, D., and Hougen, O. A., *AIChE J.* **8**, 1, 5 (1962).
7. Reid, R. C., and Sherwood, T. K., "The Properties of Gases and Liquids," 2nd ed., McGraw-Hill, New York, 1966.
8. Satterfield, C. N., "Mass Transfer in Heterogeneous Catalysis." M.I.T. Press, Cambridge, MA, 1970.
9. Richardson, J. T., *J. Catal.* **9**, 182 (1967).
10. Thomas, C. L., *Ind. Eng. Chem.* **41**, 2564 (1949).
11. Agudo, A. L., Badcock, F. R., and Stone, F. S., *Int. Congr. Catal., 4th, Moscow*, **1968**, **2**, 169 (Paper 59).